GEOMORPHIC INDICES AND FAULT SEGMENTATION INDICATION OF MENANGA FAULT AT PESAWARAN, LAMPUNG

PETUNJUK GEOMORFIK DAN INDIKASI SEGMENTASI SESAR PADA SESAR MENANGA DI PESAWARAN, LAMPUNG

Rezki Naufan Hendrawan[1*], Windi Anarta Draniswari[2], Agim Yustian Bakhtiar[3], Angga Jati Widiatama[4]

[1,3,4] Institut Teknologi Sumatera; Jalan Terusan Ryacudu, Way Huwi, Jati Agung, Lampung Selatan; 0271-8030188
[2]Badan Riset dan Inovasi Nasional; Jl. Cisitu Lama Jl. Sangkuriang, Dago, Kecamatan Coblong, Kota Bandung, Jawa Barat

How to cite this article:

Hendrawan, R.N., Draniswari, W.A., Bakhtiar, A.Y., & Widiatama, A.J. (2023). Geomorphic Indices and Fault Segmentation Indication of Menanga Fault

Abstract. Remote sensing and GIS are playing important roles in geomorphology and hazard risks analysis. Pesawaran area located near the Menanga Fault and recently on the risk of earthquake that happened along this fault. Thus, it is essential to investigate the area actively affected by Menanga Fault as preliminary research about hazard risk related to Menanga Fault. The morphometry method based on DEMNAS and Landsat 8 was applied to evaluate the zone affected by Menanga Fault, and fracture data analysis was conducted to consider the possibility of fault segmentation resulting from its mechanism. The study area can be divided into 3 zones; zone A is greatly affected by Menanga Fault activity, zone B is affected by Menanga Fault and Mt. Pesawaran development, and zone C is tectonically less affected. Zone A landforms were not only formed as a result of Menanga Thrust fault but also the strike-slip fault segment. Fault segmentation exists in this zone with different mechanisms (strike-slip and dip-slip), producing lineaments with different trends, and differentiation of river patterns.

Abstrak. Penginderaan jauh dan GIS memainkan peran penting dalam geomorfologi dan analisis risiko bahaya. Daerah Pesawaran terletak dekat dengan Sesar Menanga dan baru-baru ini berada pada risiko gempa bumi yang terjadi di sepanjang sesar ini. Oleh karena itu, sangat penting untuk menyelidiki area yang terpengaruh secara aktif oleh Sesar Menanga sebagai penelitian awal tentang risiko bahaya yang terkait dengan Sesar Menanga. Kami menggunakan

metode morfometri berbasis DEMNAS dan Landsat 8 untuk mengevaluasi zona yang terpengaruh oleh Sesar Menanga yang digabungkan dengan analisis data rekahan untuk mempertimbangkan kemungkinan segmentasi sesar dari mekanismenya. Daerah studi dapat dibagi menjadi 3 zona; zona A sangat terpengaruh oleh aktivitas Sesar Menanga, zona B terpengaruh oleh Sesar Menanga dan perkembangan Gunung Pesawaran, dan zona C kurang terpengaruh secara tektonik. Landform di zona A tidak hanya terbentuk akibat patahan celah turun Menanga tetapi juga segmen patahan celah mendatar. Segmentasi sesar ada di zona ini dengan mekanisme yang berbeda (mendatar dan turun), menghasilkan kelurusan dengan tren yang berbeda, dan diferensiasi pola sungai.

1. INTRODUCTION

Remote sensing (RS) is increasingly playing an important role in earth observation over this decade (Said & Utama, 2021). Geographic Information System (GIS) was one of the practical parts of hazard risk assessment, especially for spatial aspects, geomorphology analysis, visualization, and modelling (Ahmadi & Pekkan, 2021; Al-Ashkar et al., 2022; Moustafa et al., 2022; Ren et al., 2023; Van Westen, 2013). Digital mapping allows more efficient data collection and analysis nowadays (Fossen, 2019).

Geomorphology was a key component of hazard assessment because hazard events played a role in the dynamics of landforms and surface processes (Mohan et al., 2021; Gao et al., 2021; Van Westen, 2013; Keller & Pinter, 1996). Numerous processes affecting the dynamics of landforms and surfaces can be potentially dangerous for a human being. Those endogenic and exogenic processes can trigger hazardous processes, such as earthquakes, landslides, etc. (Keller & Pinter, 1996).

A great interest in remote sensing applications, earth dynamic modelling, and geomorphology has been observed over the past years. Previous research applied morphometry or geomorphic indices analysis on tectonically active regions, ongoing mountain building, river basins, and plate margins have been published recently (Yudhicara et al., 2017; Ganas et al., 2005; Rozycka & Migon, 2021). The remote sensing and morphometry analysis approach helps the researcher to solve the problem over the complex and weathered region. It is being a critical part of the reconnaissance phase of tectonic and/or disaster management research.

Menanga Fault was the active fault that is now believed as the source of the earthquake that happened earlier in the Pesawaran area (Nurfitriana et al., 2022). The previous study revealed that Menanga Fault was a relatively significant thrust fault (Nurfitriana et al., 2022; Mangga et al., 1993, 1994). This fault cuts through Paleozoic, Cretaceous, and Neogen Rocks. Pesawaran area is located near the shoreline and the geothermal manifestation (Haerudin et al., 2016), most of the lithology was altered (Haerudin et al., 2016), and none of the fault plane outcrops has yet been identified in this area. Besides that, it has a large population so disaster management systems were fully needed to prepare society from the hazard risks. No previous research explains the distribution of the Menanga Fault, its damage zone, and specific movement. Thus, it is essential to investigate the area actively affected by Menanga Fault by RS and GIS methods as preliminary research about hazard risk related to Menanga Fault.

This research applied the GIS method and morphometry calculation to evaluate the geomorphic indices and zone affected by Menanga Fault. Five geomorphic parameters

were assessed in this research are Bifurcation Ratio Analysis (Rb), Drainage Density (Dd), Drainage Basin Shape (Bs), Hypsometric Curves and Integral (HI), and lineament trends (Keller & Pinter, 1996; Strahler, 1952). The geomorphic indices along with the field structural data will reveal the zonation of Menanga Fault area which can be a critical part for the next disaster risk assessment of this area.

2. LITERATURE REVIEW

The study area is located in the Pesawaran region, Lampung in the vicinity of Menanga Fault. Geographically, it is situated between 105°07'30"-105°15'00" to 5°32'0"–5°35'0" (**Figure 1**). Based on the Regional Geology Map of Tanjungkarang (Mangga et al., 1993, 1994), the study area was composed of 7 rock units, from old to young aged Paleogene to Recent, there were Undifferentiated Gunung Kasih Complex (Pzg), Menanga Formation (Km), Tarahan Formation (Tpot), Sabu Formation (Tpos), Hulusimpang Formation (Tomh), Pesawaran Young Volcanic Deposits (Qhvp), and Alluvium (Qa). Menanga Formation (Km) which aged Cretaceous has structural contact with Undifferentiated Gunung Kasih Complex (Pzg) (**Figure 2**). Geological structures that formed in this area are subject to the subduction and the northern block was the moving up part of the fault.
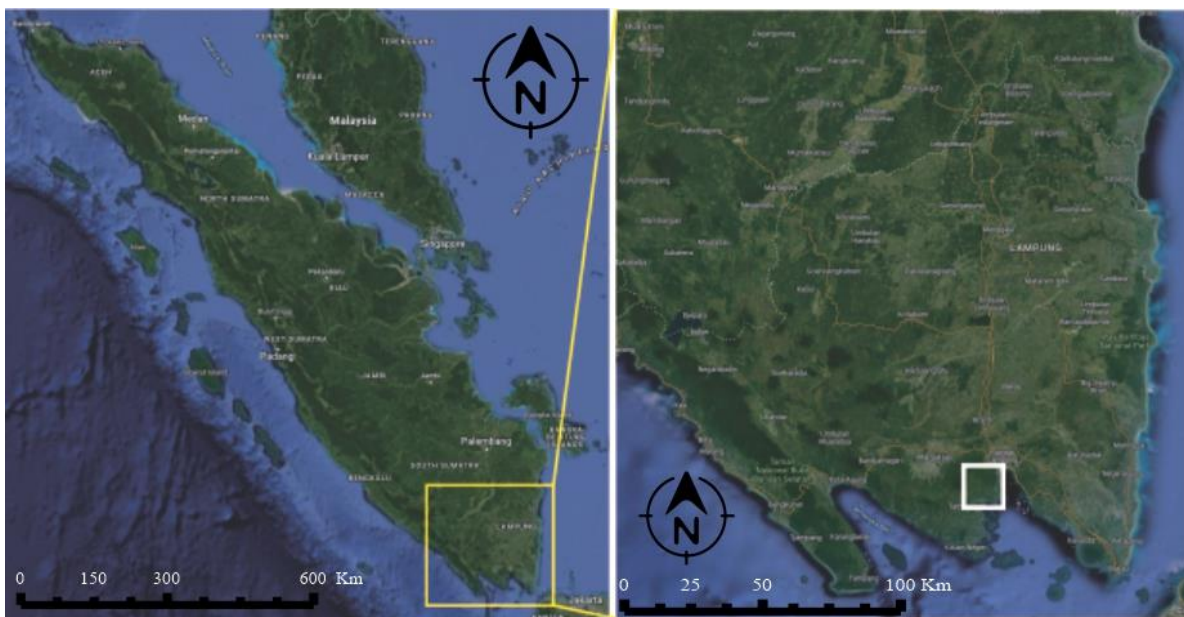

Figure 1. Location map of the study area, white box is the area of interest.
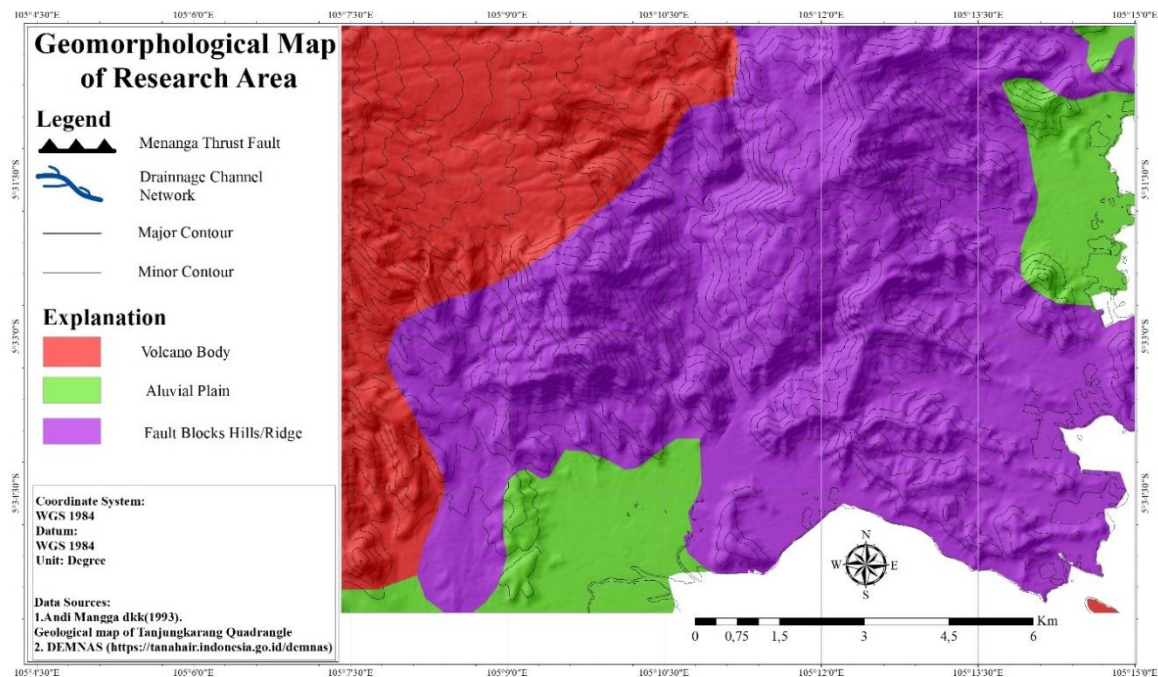
Figure 2. Geomorphological map of the research area.

3. MATERIAL AND METHODS

Digital Elevation Model Nasional (DEMNAS) with a spatial resolution of 8.25 meters and Landsat 8 taken between 2018/07/13 to 2020/08/31 with 30 meters resolution were the primary input data in this study. DEMNAS were the product combined from IFSAR data (5 meters resolution), TERRASAR-X (5 meters resolution), and ALOS PALSAR (11.25 meters resolution) from Geospatial Information Agency (BIG) Indonesia. Regional geology data as the basic regional framework was taken from the regional geological map of Tanjungkarang (Mangga et al., 1993).

Lineament delineation, hill shade analysis, watershed analysis, and morphometry parameter quantification carried out using ArcGIS 10.8 software and Microsoft Excel. The ArcGIS processing was completed with white box tools for hypsometric analysis. QGIS and Semi-Automatic Classification Plugin were used in this research for atmospheric correction, clipping, and band composite of Landsat 8. Lineament extraction was applied in

RGB band composite 5, 8, 2 (Misra et al., 2020; Taoufik et al., 2016). In addition, PCI Geomatica 2018 was used to delineate the contour from hill shades and Landsat 8 automatically. This research includes the studio project for remote sensing and GIS analysis through the software mentioned before, a field visit, and a comprehensive analysis of stress. The GIS analysis was validated based on a field visit and geomorphological observation. Besides the geomorphological observation, shear fracture data were used for validation. The stress analysis of shear fracture data was done using WinTensor 4.0.3.

4. RESULT AND DISCUSSION

Geomorphological map the of research area (**Figure 2**) presented 3 different geomorphology units. This location consists of a volcanic body in the western area along north to south, a fault block ridge in center area, and an alluvial plain. This phenomenon indicated that located composed of different endogenous aspects.

The area of interest is divided into 16 watersheds (DAS) and 6 river patterns; parallel in DAS 1, 3, 9, 10, 11, 15, and 16, sub-parallel in DAS 4, 6, 7, and 13, rectangular in DAS 8 and 14, dendritic in DAS 5, sub-dendritic in DAS 2, and pinnate in DAS 12 (**Figure 3**). The morphometric calculation was done for all watersheds. The bifurcation ratio (Rb) is the ratio number of river segments in each watershed that reflects the branching of the river (Keller & Pinter, 1996). The more actively tectonic a zone, the higher number of Rb in a watershed. Rb of 16 watersheds is ranging from 1.04 to 6.35. Basin shape (Bs) value defines the planimetric shape of a basin (Keller & Pinter,

1996; Yudhicara et al., 2017). High Bs values provide the elongated basin and higher tectonic activity than the low Bs value. Bs value of 16 watersheds are ranging from 0.27 to 9.67. Drainage density (DD) defines the amount of water stored in a catchment area (Keller & Pinter, 1996). DD number or the research area is ranging from 2.36-4.74. Hypsometric Curve and Integral (HI) show the elevation distribution that defines the stadium of morphology (Keller & Pinter, 1996). HI of the research area ranging from 0.19-0.56. HI describes the geomorphic condition quantitatively. Old geomorphic stadium tends to have HI<0.4 while 0.4<HI<0.6 is interpreted as mature geomorphic (Strahler, 1952).

Figure 3. Geological map of the research area and its watershed delineation (Modified from Mangga et al., 1993).

The study area has two different geomorphic stadiums. Northern and northwest area are belonging to mature stadium while the eastern and southeast areas is old stadiums. The data obtained from morphometry calculation cannot be directly interpreted to divide the tectonic affected zone. It is essential to make spatial observations to see the pattern of significant changes. Interpolation is performed by using Inverse Distance Weighting (IDW) and contouring methods to help the data

visualization and compared with Landsat. This visualization (**Figure 4**) then compared to the lineament taken from Landsat for further interpretation.

In general, the morphometry analysis from the parameters above shows that there are 2 zone, the eastern block and the western block. Looking into more detail, the eastern block can be divided into two other zones as it tends to have different patterns of the lineament and morphometric range values in the north and

south. Thus, there are 3 zones with different structural effects in the research area, those three zones are Zone A, Zone B, and Zone C (**Figure 5**). The drainage bifurcation ratio (Rb) shows that Zone A has a greater value than Zone B and C so it can be interpreted that the most significant level of fault activity is located in Zone A (**Table 1**).
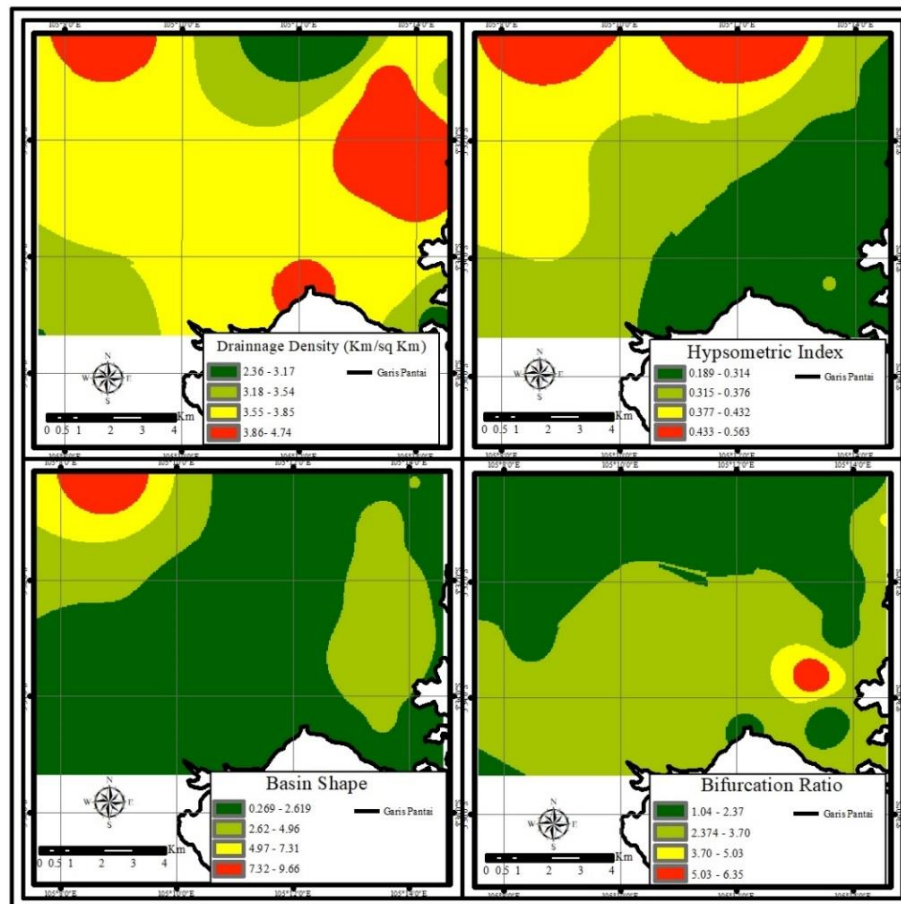

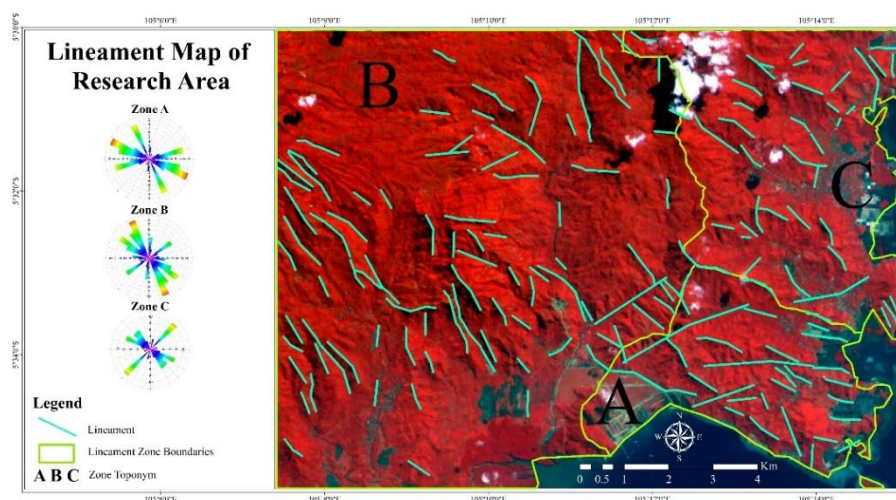
Figure 4. Contouring map of the morphometry parameters.

Figure 5. Lineament map of the research area.

Table 1. Zone Classification.

Morphometric Parameters	Zone A	Zone B	Zone C
	DAS 2, 8, 11, 13	**DAS 7, 9, 10, 12, 16**	**DAS 1, 3, 4, 5, 6, 14, 15**
Bifurcation Ratio (Rb)	1.64-6.36	1.04-3.70	1.44-3.79
Basin Shape (Bs)	0.7-3.7	1.34-9.67	0.27-3.30
Drainage Density (DD)	3.06-3.97	3.16-4.08	2.36-4.74
Hypsometric Curves and Integral (HI)	0.19-0.32	0.35-0.47	0.25-0.56
Lineament	NW-SE, NE-SW	NW-SE	NE-SW
Geological Interpretation	Greatly affected by Menanga Fault	Affected by Menanga Fault and Mt. Pesawaran	Less Affected by Menanga Fault
Slope class	Gently slope (2-7%) – Steep (30-70%)	Moderately Steep (15-30%) – Very Steep (70-140%)	Flat – Moderately Steep (0-30%)

Lineament data from band 5, 8, and 2 RGB composite generally show NW-SE trending, but there are different patterns between zone A and B (**Figure 5**). Zone A is dominated by both NW-SE and NE-SW trends. Based on the cross-cutting relationship, NW-SE trends are cut through NE-SW trends. Compared with the regional geology maps, those NW-SE trends are defined as Menanga Fault. On the other hand, based on remote sensing analysis, Zone B has dominant NW-SE lineament trends. Based on those trends, supported by morphography and lithology distribution, the fault activities in this zone are not only affected by Menanga Fault but also volcanic process of Mt. Pesawaran which has eruption centre in the northwest part of the study area. Zone C in the northern part of the research area tends to have a NE-SW lineament pattern with less quantity of lineament. Zone C is relatively less affected by Menanga Fault.

The analysis is reinforced by six fractures as field data that were found in several areas representing each zone (green circle in **Figure 5**). Field data of zone A show shear fractures with a couple of plane directions (**Figure 6**) which are thought to have been formed due to the activity of the Menanga Fault. Rose diagrams of A.1 and A.2 revealed NW-SE and NE-SW trending, in line with the result of remote sensing analysis. The most striking feature is, even in stations affected by Menanga Fault, the stress pattern implied a different system based on Anderson's model (Anderson, 1951; Fossen, 2016), A.1 in the southeast area showed a strike-slip pattern with both maximum and minimum stress in the horizontal axis while A.2 indicated a dip-slip pattern with minimum stress presented on the vertical axis. The pattern of stress tend to be sinistral strike-slip movement.
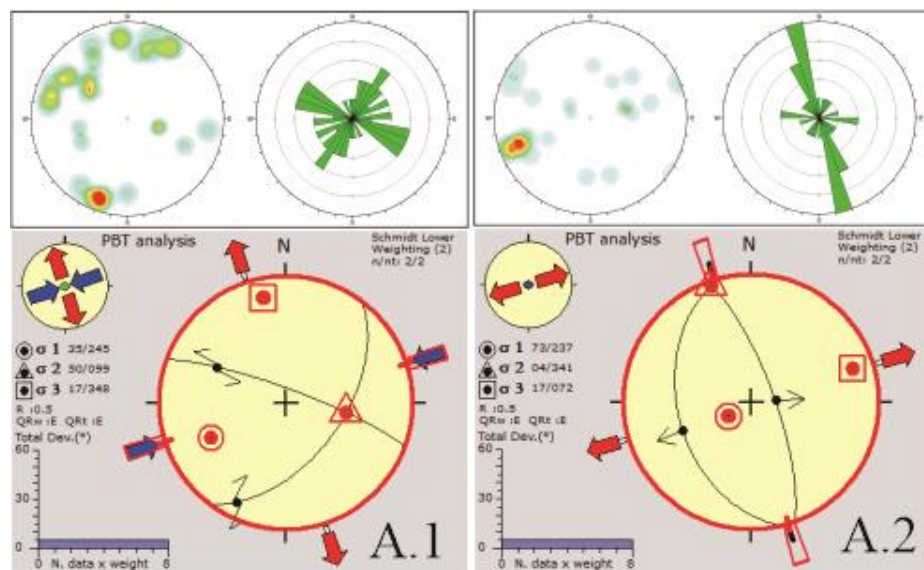
Figure 6. Stereograph analysis of the shear fracture data from stations A.1 and A.2.

The analysis is reinforced by six fractures as field data that were found in several areas representing each zone (green circle in **Figure 5**). Field data of zone A show shear fractures with a couple of plane directions (**Figure 6**) which are thought to have been formed due to the activity of the Menanga Fault. Rose diagrams of A.1 and A.2 revealed NW-SE and NE-SW trending, in line with the result of remote sensing analysis. The most striking feature is, even in stations affected by Menanga Fault, the stress pattern implied a different system based on Anderson's model (Anderson, 1951; Fossen, 2016), A.1 in the southeast area showed a strike-slip pattern with both maximum and minimum stress in the horizontal axis while A.2 indicated a dip-slip pattern with minimum stress presented on the vertical axis. The pattern of stress tend to be sinistral strike-slip movement.

Move to field data from zone B, B.1 is shear fractures that have two dominance fractures trends, NE-SW and NW-SE (**Figure 7**). The shear fractures are dip-slip but the other one (B.2) is tension joints with only one dominant trending, thus these kinds of tension are not the product of Menanga Fault activity but are interpreted as formed by the growth of Mt.Pesawaran. The last zone is zone C, overall, the data shows only 1 major trend which is NE-SW thus it was not shear fracture related to tectonics but non-tectonically related fractures in the form of tension joints. The data from zone C are displayed as a rosette diagram only due to its type of tension joint (**Figure 8**).

In sum up, based on both GIS and field data, it can be interpreted that Menanga Fault was a major active tectonic process that affected the landform formation but it was not the only process affecting its adjacent area. The zone that was greatly affected by Menanga Fault was zone A. The landform formation in the research area is not only affected by Menanga Fault but also formed by the growth of Mt.Pesawaran and other fault segments. Fault segmentation exists in this zone with different mechanisms (strike-slip and dip-slip), producing lineaments with different trends, and differentiation of river patterns. Fault segmentation corresponds with the different mechanisms in the nearby area as shown by the stereograph analysis of the fracture. This research is limited in asses the indication of fault segmentation, yet describes its boundary.
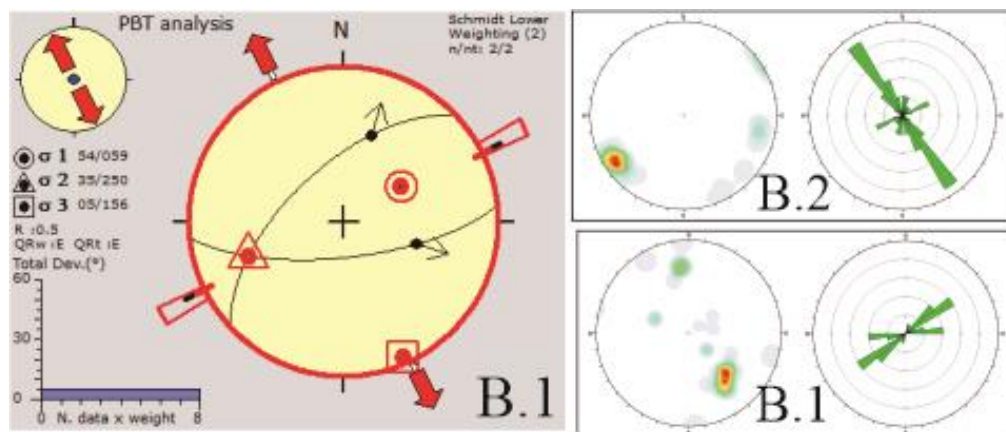
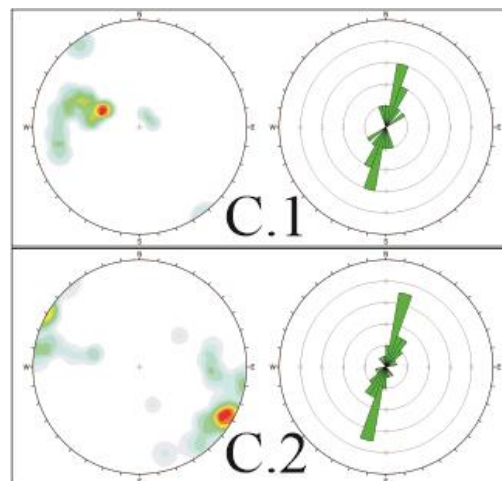**Figure 7.** Stereograph analysis of the fracture data from station B.1 and B.2.

Figure 8. Rossete diagrams of the fracture data
from station C.1 and C.2.

5. CONCLUSION

GIS processing and geomorphic indices calculation are suitable to evaluate the actively tectonic affected zone of Menanga Fault. The Pesawaran area can be divided into three zones, zone A located in the southeast greatly affected by Menanga Fault, zone B in the west is affected by both Menanga Fault and Mt. Pesawaran, while zone C is tectonically less affected. Furthermore, this study found the possibility of Menanga Fault segmentation that there are dip-slip faults and strike-slip faults in this area. Further research is recommended to consider the movement of each fault segment. It will be useful for the assessment of seismic hazards in the next steps because possibly the segmentation boundary behaves as the main point of shocks or rupture.

AUTHOR CONTRIBUTION

RNH performed the conceptualization, GIS processing, data interpretation, analysis, and wrote the manuscript, WAD performed the data interpretation, analysis, and wrote the manuscript, AYB performed the GIS processing, layouting, and wrote the manuscript, AJW performed the geological data for validation and wrote the manuscript.

REFERENCES

Ahmadi, H., & Pekkan, E. (2021). Fault-Based Geological Lineaments Extraction Using Remote

Sensing and GIS—A Review. *Geosciences.* https://www.mdpi.com/1085090

Al-Ashkar, A., Schlupp, A., Ferry, M., & Munkhuu, U. (2022). Tectonic Geomorphology and Paleoseismology of The Sharkhai Fault: A New Source of Seismic Hazard for Ulaanbaatar (Mongolia). *Solid Earth.* https://se.copernicus.org/articles/13/761/2022/

Anderson, E. (1951). *The Dynamic of Faulting.* Edinburgh: Oliver & Boyd.

Fossen, H. (2016). *Structural Geology 2nd edition.* United Kingdom: Cambridge University Press.

Fossen, H. (2019). Writing Papers with An Emphasis on Structural Geology and Tectonics: Advices and Warnings. *Brazilian Journal of Geology,* 49(4). https://doi.org/10.1590/2317-4889201920190109

Ganas, A., Pavlides, S., & Karastathis, V. (2005). DEM-based Morphometry of Range-Front Escarpments in Attica, Central Greece, and Its Relation to Fault Slip Rates. *Geomorphology.* 65(3-4).

Gao, K., Huang, L., & Zheng, Y. (2021). Fault Detection on Seismic Structural Images Using A Nested Residual U-Net. *Geoscience and Remote Sensing.* https://ieeexplore.ieee.org/abstract/document/9418625/

Haerudin, N., Karyanto, & Kuntoro, Y. (2016). Radon and Thoron Mapping to Delineate The Local-Fault in The Way Ratai Geothermal Field Lampung Indonesia. *Journal of Engineering and Applied Sciences.* 11(7). 4804-4809.

Keller, E, A., & Pinter, N. (1996). *Active Tectonics: Earthquakes, Uplift, and Landscape.* Prentice Hall.

Mangga, S., Amirudin, Suwarti, T., Gafoer, S., & Sidarto. (1993). *Peta Geologi Lembar Tanjung Karang.* Bandung: Badan Geologi.

Mangga, S., Amirudin, Suwarti, T., Gafoer, S., & Sidarto. (1994). *Geologi Lembar Tanjung Karang.* Bandung: Badan Geologi.

Misra, A., Agarwal, K. K., Kothyari, G. C., Talukdar, R., & Joshi, G. (2020). Quantitative Geomorphic Approach for Identifying Active Deformation in The Foreland Region of Central Indo-Nepal Himalaya. *Geotectonics.* https://doi.org/10.1134/S0016852120040093

Mohan, Amrita & Singh, Amit & Kumar, Basant & Dwivedi, Ramji. (2021). Review on Remote Sensing Methods for Landslide Detection Using Machine and Deep Learning. *Transactions on Emerging Telecommunications Technologies.* 32. 10.1002/ett.3998.

Moustafa, S. S. R., Abdalzaher, M. S., & Abdelhafiez, H. E. (2022). Seismo-Lineaments in Egypt: Analysis and Implications for Active Tectonic Structures and Earthquake Magnitudes. *Remote Sensing.* https://www.mdpi.com/1986470

Nurfitriana, I., Nugraha, P., Wulandari, R., Fattah, E. I., & Wibowo, A. (2022). Identification of the Existence of Inferred Menanga Fault based on Gravity Anomaly, Pesawaran, Lampung. *Proceedings of the Soedirman International Conference on Mathematics and Applied.* 5, 78-83.

Ren, Z., Zhang, P., Oguchi, T., & He, Z. (2023). Remote Sensing Perspectives on Geomorphology and Tectonic Processes. *Remote Sensing.* https://www.mdpi.com/2072-4292/15/9/2327

Rozycka, M., & Migon, P. (2021). Morphometric Properties of River Basins as Indicators of Relative Tectonic Activity – Problems of Data Handling and Interpretation. *Geomorphology.* 389.

Said, Y.M. & Utama, H.W. (2021). Analysis of The Physical Morphology of The Jambi Masurai Caldera Using High Resolution Satellite Image. *JGE (Jurnal Geofisika Eksplorasi),* 07(03), 178-190.

Strahler, A. (1952). Hypsometric (Area-Altitude) Analysis of Erosional Topography. *Bulletin of the Geological Society of America.* 63(11), 1117-1142.

Taoufik, M., Baghdad, B., El Hadi, H., & Laghlimi, M. (2016). Structural Interpretation of Lineaments by Remote Sensing and GIS using Landsat 8 Data: A Case Study of Akreuch Area (Morocco). *European Journal of Scientific Research.* 138. 216-224.

Van Westen, C. J. (2013). Remote Sensing and GIS for Natural Hazards Assessment and Disaster Risk Management. *Elsevier Ltd,* vol.3.

Yudhicara, Muslim, D., & Sudradjat, A. (2017). Geomorphic Analysis in Determining Tectonic Activity Affected by Sumatra Fault in Liwa Region and Its Surrounding Area, Lampung, Indonesia. *Indonesian Journal on Geoscience.* 4(3), 193-208.